Models and Methods of Simulating Gas Pipeline Blowdown

K.K. BOTROS, W.M. JUNGOWSKI, and M.H. WEISS

Nova Husky Research Corp., 2928 - 16 Street N.E., Calgary, Alberta, T2E 7K7

Estimation of gas pipeline blowdown time requires the determination of the pressure-time history for the unsteady discharge of gas through a blowdown stack open to the atmosphere. Computational procedures entail various assumptions whose validity and contributions to the accuracy are often not assessed. This paper discusses the computational models and solution methods and further assesses the significance of the various assumptions involved.

Volume and pipe models, numerical and analytical methods of solution, effects of stack entrance and friction losses and discharge coefficient are evaluated. The accuracy of a particular model or method of solution is greatly dependent on the fL/D ratio of the pipe section under blowdown. Comparison with field measurements of a straight pipe section and a complicated compressor station yard piping enabled evaluation of the above models.

Afin d'estimer le temps de chasse d'une conduite de gaz, il est nécessaire de déterminer la relation pression-temps pour la décharge en régime instationnaire du gaz dans une cheminée de vide-vite ouverte sur l'atmosphère. Les méthodes de calcul par ordinateur fournissent des hypothèses émises.

Les modèles de volume et de conduite, les méthodes de résolution numériques et analytiques, les effets de l'entrée de la cheminée et des pertes par friction ainsi que le coefficient de décharge sont évalués. L'exactitude d'un modèle particulier ou d'une méthode de résolution dépend fortement du rapport fL/D de la section de conduite sous vide-vite. Les modèles ci-dessus ont pu être évalués par comparaison avec les mesures de champ d'une section de conduite droite et d'une tuyauterie d'une station complexe de compresseurs.

Keywords: gas pipeline blowdown, pipeline transient, unsteady flow, blowdown simulation.

Evacuation of a gas pipeline occurs during blowdown or after rupture of a pipeline element. In the first case the exit cross-sectional area of the riser is much smaller than that of the main pipe. Consequently, the gas velocity in the pipeline is typically about 10 - 30 m/s during sonic discharge and the flow can be regarded as quasi-steady. Stagnation pressure at the stack exit, which determines the discharge flux to the atmosphere, is a function of pipeline pressure at the stack entrance and pressure losses in the riser. In case of a rupture, however, the exit area can be as large as the main pipe cross-sectional area and thus flow velocity in the pipe becomes high (about 350 m/s initially at the ruptured section) and varies rapidly with time. The above comparison indicates that the two cases require different physical models and mathematical descriptions for the calculation of pressure-time history during evacuation of the pipeline. This study is restricted to blowdown only.

The schematic in Figure 1 shows a blowdown riser at the end of a pipeline section. The internal flow during sonic discharge from the stack occurs with low velocity in the main pipe, moderate velocity along L_{s1}, sonic velocity at the valve throat and mostly supersonic velocity along L_{s2} and at the exit. This pattern can be attributed to a typical stack with a plug valve. The geometry of such a stack is characterized by the effective cross-sectional area ratio of the valve throat to the stack being equal to about 0.6 and L_{s2}/D_s being less than 10. After an abrupt enlargement of the duct cross-section downstream of the throat, a supersonic flow with oblique shock waves occurs until the main pipe pressure falls to a level approximately 2.5 times the ambient pressure (Jungowski, 1968; Anderson and Meier, 1982). With further decrease in the main pipe pressure, a subsonic flow is established along L_{s2}, and soon after, the sonic discharge is terminated when the pipe pressure drops approximately below 1.5 times the ambient pressure. Due to the pressure recovery downstream of the throat, the pipe pressure terminating the sonic discharge is lower than that with $L_{s2} = 0$ when no pressure recovery takes place and as a result, the duration of sonic venting is extended. The friction losses along L_{s2} do not affect the flow rate during sonic discharge but slightly raise the pipe pressure at which this phase is terminated. However, during the subsonic discharge obviously these losses decrease the flow rate and hence slow down the discharge process. It seems that these opposite effects, i.e. faster discharge due to extension of sonic venting and slower discharge during the subsonic phase, allow for a simplification to regard the valve throat as an exit to the ambient pressure. Therefore, this simplification was applied to all models and methods of solution discussed in this paper.

Generally, the flow pattern along L_{s2} depends on throat/stack area ratio, the pipe pressure and whether $(fL_{s2}/D_s) \lessgtr (fL_{s2}/D_s)_{max}$ (Shapiro, 1953). These factors determine flow at the exit, $M_e \gtrless 1$. For the stack characterized above, $(fL_{s2}/D_s) < (fL_{s2}/D_s)_{max}$. However, with abnormally long L_{s2} or different area ratio, the flow may be choked at the exit but not at the valve throat. In that case the downstream friction losses such as those along L_{s1} will decrease the flow rate during the sonic discharge.

Accuracy in predicting the blowdown time is determined by proper description of thermo- and gas dynamic behavior of gas during this unsteady process. Specifically, gas expansion in the pipe and at the throat and precise determination of friction losses in the riser and of throat discharge coefficient, are of particular importance. Pressure losses depend on L/D, L_{s1}/D_s, L_{s2}/D_s, shape of the riser inlet and roughness of the main pipe and the riser. It is expected that stack friction losses can extend the blowdown time by about 5 to 10% (Gradle, 1984).

The literature related to blowdown time prediction is rather scarce (Gradle, 1984) contrary to many papers dealing with slow (Osiadacz, 1984; Streeter and Wylie, 1970; Rachford and Dupont, 1974) or fast transients (Flatt, 1986; Cronje et al., 1980; Groves et al., 1978; Picard and Bishnoi, 1988) in gas pipeline systems.

In this paper two physical models are described; the pipeline section is regarded either as a *volume* with stagnation conditions inside or as a *pipe* with velocity increasing towards the exit. Solutions of the pertinent equations for each model

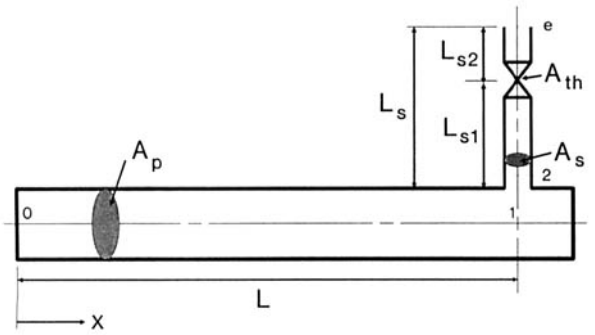

Figure 1 - Schematic of a blowdown section.

were obtained *analytically* for natural gas with some reference gas paramenters and *numerically* taking into account the real gas properties at each time step during blowdown. Effects of friction losses in the riser upstream of the throat were also considered in the numerical methods. Calculated blowdown times were compared with those obtained using graphs of Gradle (1984) and own field measurements of a straight pipe section and a compressor station yard piping.

Gas expansion in the main pipe generally is regarded as an isothermal process because the shortest blowdown lasts at least a couple of minutes during which heat transfer to the gas occurs. Thermal capacitance of the pipe and surrounding soil secures sufficient heat flow to prevent much change in the gas temperature. To assess this assumption the gas temperature was measured and calculated during the blowdown of a compressor station piping. The lowest temperature measured was slightly below freezing and the one calculated with a steady heat transfer model was −12°C. Nevertheless, the pressure-time profile calculated for the latter case was very close to that calculated for the isothermal process. In reality, the lowest temperature most probably was below the measured one due to some thermal inertia of the thermometer housing but above the calculated temperature due to the enhanced heat transfer with a transient temperature distribution in the soil. If contents of the heaviest gas components are not exceeding the specification gas requirements, condensation should not occur above −10°C and therefore it seems that typically there is no need to take it into account. During the isentropic gas expansion at the throat the gas temperature is lowered considerably, but due to the relaxation time condensation should not affect the process of expansion and thus the flow rate.

Volume Model

This model neglects the effects of flow and friction along the main pipe and hence assumes that stagnation conditions prevail inside the whole pipe section under blowdown. Isothermal gas expansion is assumed inside the main pipe and isentropic flow through the stack.

Mass conservation requires that

$$G dt = -V d\rho \quad \ldots\ldots (1)$$

The equation of state of the gas has the form:

$$\rho = \rho(P, T) \quad \ldots\ldots (2)$$

The procedures describing the analytical and the numerical solutions of these equations are given below.

Analytical Volume Solution

For perfect gas and T = constant, Equation (2) yields

$$d\rho = dP / RT \quad \ldots\ldots (3)$$

and thus Equation (1) can be transformed into

$$GRTdt = -V \cdot dP \quad \ldots\ldots (4)$$

For sonic flow at the valve throat and assuming isentropic expansion from the pipe stagnation conditions, the mass flow rate (Shapiro, 1953) is:

$$G_c = \left[\frac{2}{k+1}\right]^{\frac{k+1}{2(k-1)}} \left[\frac{k}{RT}\right]^{\frac{1}{2}} P \cdot A_{th} \cdot C_d \quad \ldots\ldots (5)$$

where the discharge coefficient C_d depends on the type of the valve.

The time constant τ_v is defined as:

$$\tau_v = \frac{V\left[\frac{k+1}{2}\right]^{\frac{k+1}{2(k-1)}}}{c \cdot A_{th} \cdot C_d} \quad \ldots\ldots (6)$$

where c is the speed of sound ($c = \sqrt{kRT}$). Introducing Equations (5) and (6) in the original Equation (4) yields the normalized differential equation:

$$d\bar{t}_c = -d\bar{P} / \bar{P} \quad \ldots\ldots (7)$$

where the normalized pressure $\bar{P} = P/P_a$, P_a is the ambient pressure and time $\bar{t} = t/\tau_v$.

After integration from initial pressure $\bar{P}_i$ to the pressure $\bar{P}_c$, which terminates sonic flow, one obtains the time of sonic venting as:

$$\bar{t}_c = \ln\bar{P}_i - \ln\bar{P}_c \quad \ldots\ldots (8)$$

or taking into account that

$$\bar{P}_c = \left[\frac{k+1}{2}\right]^{\frac{k}{(k-1)}} \quad \ldots\ldots (9)$$

then, the dimensionless time for the sonic venting can be written as;

$$\bar{t}_c = \ln\bar{P}_i - \left[\frac{k}{k-1}\right]\ln\left[\frac{k+1}{2}\right] \quad \ldots\ldots (10)$$

Generally, the pressure-time history during sonic venting can be determined from Equation (8) as:

$$P / P_i = \exp(-\bar{t}) \quad \ldots\ldots (11)$$

where $0 < \bar{t} < \bar{t}_c$. This indicates that the pressure drop in the main pipe occurs exponentially during sonic venting.

Following the sonic venting is a subsonic discharge where the critical flow pressure corresponding to the line stagnation pressure is less than the ambient pressure P_a. During this period, the mass flow rate can be expressed as:

$$G_s = \left[\frac{2}{k-1}\right]^{\frac{1}{2}} \left[\frac{k}{RT}\right]^{\frac{1}{2}} \left[\bar{P}^{-\frac{2}{k}} - \bar{P}^{-\frac{k+1}{k}}\right]^{\frac{1}{2}} P \cdot A_{th} \cdot C_d \quad \ldots\ldots (12)$$

TABLE 1
Solution of Equation (14) for Subsonic Venting Time

		$N(k,\bar{P}_b)$			$\bar{t}_s$		
		$\bar{P}_b$			$\bar{P}_b$		
k	$\bar{P}_c$	1.1	1.01	1.001	1.1	1.01	1.001
1.3	1.8324	2.5525	3.4560	3.7406	0.5785	0.7833	0.8479
1.314	1.8409	2.5233	3.4108	3.6907	0.5842	0.7897	0.8545
1.35	1.8627	2.4585	3.3100	3.5787	0.5985	0.8058	0.8712
1.4	1.8929	2.3883	3.1987	3.4546	0.6181	0.8278	0.8941

Introducing Equation (12) into Equation (4) and following the previous transformations we obtain the differential equations:

$$d\bar{t} = \frac{\left[2^{\frac{1}{k-1}}(k-1)^{\frac{1}{2}}/(k+1)^{\frac{k+1}{2(k-1)}}\right]d\bar{P}}{\left[\bar{P}\left(\bar{P}^{-2/k} - \bar{P}^{-(k+1)/k}\right)\right]} \quad \ldots\ldots\ldots (13)$$

Numerical integration from $\bar{P}_c$ to $\bar{P}_b$ yields the time of subsonic venting

$$\bar{t}_s = 2^{1/(k-1)}(k-1)^{1/2}/(k+1)^{(k+1)/2(k-1)} N(k, \bar{P}_b) \quad \ldots\ldots\ldots (14)$$

where $N(k, \bar{P}_b)$ denotes the value of the integral and $\bar{P}_b > 1$. The effect of k and $\bar{P}_b$ on $\bar{t}_s$ is shown in Table 1.

The total normalized time of blowdown from $\bar{P}_i$ to $\bar{P}_b$ will then be

$$\bar{t}_b = \bar{t}_c + \bar{t}_s \quad \ldots\ldots\ldots (15)$$

or in seconds

$$\bar{t}_b = \bar{t}_b \cdot \tau_v \quad \ldots\ldots\ldots (16)$$

Numerical Volume Solution

In the above analytical solution, the gas properties needed for the analysis, namely k and c, were assumed constant for the duration of the blowdown and were calculated at a reference pressure and temperature (averaged throughout the process) from an equation of state. This is rather a necessary assumption if a closed form analytical solution is required. In order to account for variations in gas properties as conditions change in the pipe volume, numerical methods are necessary. An appropriate equation of state such as the BWRS or AGA-8 equations, is needed to provide not only the P-ρ-T relation [Equation (2)] but also the derived thermodynamic properties required for the numerical computation. The mass conservation equation, Equation (1), is still valid, and the assumptions of isothermal expansion of the gas inside the pipe volume and isentropic flow through the stack (adiabatic flow with no losses) still apply.

For *sonic discharge*, Equation (1) can be written as:

$$V\frac{d\rho}{dt} = -(\rho_{th} \cdot c_{th} \cdot A_{th} \cdot C_d) \quad \ldots\ldots\ldots (17)$$

where subscript 'th' refers to throat condition, and

$$\rho_{th} = \rho(P_{th}, T_{th})$$

$$c_{th} = c(P_{th}, T_{th})$$

are determined from the state equation. The throat pressure and temperature (P_{th}, Tt_h) are related to the pressure and temperature of the gas in the pipe volume (P, T) and can be calculated from the state equation using an iterative procedure for isentropic expansion to sonic conditions. Additionally, the thermodynamic relation:

$$\left(\frac{\partial P}{\partial \rho}\right)_T = \left(\frac{\partial P}{\partial \rho}\right)_s / \gamma = c^2/\gamma \quad \ldots\ldots\ldots (18)$$

is used to describe the isothermal expansion of the gas inside the pipe volume, where γ is the specific heat ratio. Hence Equation (17) can be written as:

$$\frac{\gamma V}{c^2}\frac{dP}{dt} = -\rho_{th}c_{th}A_{th}C_d = f_c(P,T) \quad \ldots\ldots\ldots (19)$$

Equation (18) is also used to calculate the speed of sound c from the equation of state.

For *subsonic discharge*, i.e. when the critical flow pressure is less than the ambient pressure, Equation (19) is replaced by

$$\frac{\gamma V}{c^2}\frac{dP}{dt} = -\rho_{th}u_{th}A_{the}C_d \quad \ldots\ldots\ldots (20)$$

where: $\rho_{th} = \rho(P_a, T_{th})$

u_{th} = throat velocity calculated from the isentropic expansion from the pipeline volume conditions (P,T) to the ambient pressure P_a.

This also requires an iterative procedure since the R.H.S. of Equation (20) is also a function of the pressure and temperature in the pipe volume, i.e.

$$\frac{\gamma V}{c^2}\frac{dP}{dt} = -\rho_{th}u_{th}A_{th}C_d = f_s(P,T) \quad \ldots\ldots\ldots (21)$$

Both Equation (19) and Equation (21) are quasi-linear, ordinary differential equations of the first order and were solved numerically using the variable order Backward Differentiation Formula (BDF) method known as Gear's method (Harwell Subroutine Library - DC03 Routine, 1988). The iterative procedures involved in the isentropic expansion of the gas to the stack throat are quite intensive particularly with the **AGA-8** state equation whose coefficients are temperature dependent. For this reason, the **BWRS** state equation was used in the present analysis and in all of the results presented in this paper. Comparison of these equations of state performed by Studzinski et al. (1988) for isentropic expansion of the gas to critical flow conditions, however, revealed that

the difference between the two equations in enthalpy prediction lies between 1-2%.

Pipe Model

This model takes into account flow velocity and friction losses along the main pipe section under evacuation. The other assumptions are the same as for the volume model, i.e. isothermal expansion of the gas in the main pipe and isentropic through the stack.

The one-dimensional flow along the pipe is described by the continuity equation

$$\frac{\partial \rho}{\partial t} + \frac{\partial(\rho u)}{\partial x} = 0 \quad \ldots\ldots\ldots\ldots\ldots\ldots\ldots\ldots (22)$$

the momentum equation

$$\frac{\partial u}{\partial t} + u\frac{\partial u}{\partial x} + \frac{1}{\rho}\frac{\partial P}{\partial x} + fu^2 / 2D = 0 \quad \ldots\ldots\ldots\ldots (23)$$

and the gas state equation, Equation (2).

Analytical Pipe Solution

As in the previous analytical solution for the volume model, a closed form solution is only possible with ideal gas behavior, i.e. $P = \rho RT$. Introduction of the gas flux $Q = \rho u$ as a variable, linearization of the resistive term

$$fu^2 / 2D = (fu / 2D)_{av} \cdot u = a\,u \quad \ldots\ldots\ldots\ldots\ldots\ldots (24)$$

where a is the attenuation factor, and omission of the inertial terms in Equation (23) results in the modified equations of continuity:

$$(1 / RT)\frac{\partial P}{\partial t} + \frac{\partial Q}{\partial x} = 0 \quad \ldots\ldots\ldots\ldots\ldots\ldots\ldots (25)$$

and momentum:

$$\frac{\partial P}{\partial x} + a\,Q = 0 \quad \ldots\ldots\ldots\ldots\ldots\ldots\ldots\ldots (26)$$

Differentiating Equation (26) with respect to x and subtracting from Equation (25) yields

$$\frac{\partial P}{\partial t} = \kappa\frac{\partial^2 P}{\partial x^2} \quad \ldots\ldots\ldots\ldots\ldots\ldots\ldots\ldots (27)$$

where

$$\kappa = \frac{RT}{a} \quad \ldots\ldots\ldots\ldots\ldots\ldots\ldots\ldots\ldots (28)$$

The partial differential equation, Equation (27), describing a slowly varying flow in the main pipe, is linear, parabolic and of the second order and is known as the one-dimensional heat conduction equation (Carslaw and Jaeger, 1959). This equation can be solved once the boundary and initial conditions for the pipeline are specified. At the closed end, $x = 0$ (Figure 1), $Q = 0$ prevails at all times and thus from Equation (26), $\partial P/\partial x = 0$. At the stack end, $x = L$, and during sonic venting the gas flux is proportional to the pipe pressure, i.e. $Q = EP$ [see Equation (5)] where E is a constant. At the beginning of blowdown the pressure in the entire pipeline is equal to P_i, thereby setting the initial conditions.

To solve this boundary value problem the method of separation-of-variables (Carslaw and Jaeger, 1959) was applied and the solution of Equation (27) is given by

$$P(x, t) = [\,A\cos(\lambda x) + B\sin(\lambda x)\,]\exp(-\kappa\lambda^2 t) \quad \ldots\ldots (29)$$

Differentiation of Equation (29), and introduction of the boundary condition at $x = 0$ results in $B = 0$ and hence

$$P(x, t) = A\cos(\lambda x)\exp(-\kappa\lambda^2 t) \quad \ldots\ldots\ldots\ldots\ldots (30)$$

The boundary condition at $x = L$ yields from Equation (26):

$$\frac{\partial P(L, t)}{\partial x} + a\,E\,P\,(L, t) = 0 \quad \ldots\ldots\ldots\ldots\ldots (31)$$

After introduction of Equation (30) we get

$$\alpha\tan(\alpha) = a\,E\,L \quad \ldots\ldots\ldots\ldots\ldots\ldots\ldots (32)$$

where $\alpha = \lambda L$.

The initial conditions will be fulfilled if the solution can be developed in an infinite series as

$$P(x, t) / P_i = \sum_{n=1}^{\infty} A_n \cos(\alpha_n x / L)\exp(-\kappa\alpha_n^2 t / L^2) \quad \ldots (33)$$

The coefficients A_n can be calculated from the relation

$$A_n = \int_o^L \cos\left(\alpha_n \frac{x}{L}\right)dx \Big/ \int_o^L \cos^2\left(\alpha_n \frac{x}{L}\right)dx \quad \ldots\ldots (34)$$

and after integration

$$A_n = 4\sin\alpha_n / (2\alpha_n + \sin 2\alpha_n) \quad \ldots\ldots\ldots\ldots (35)$$

Table 1 of Appendix IV in Carslaw and Jaeger (1959) indicates that for $aEL < 0.1$ the second root α_2 of Equation (35) is greater than ten times the first root α_1 and thus the series is rapidly converging. In this range A_1 is also very close to unity ($A_1 = 1.016$ for $aEL = 0.1$). With decreasing aEL, the coefficient A_1 tends to unity and the higher A_n coefficients tend to zero. According to Equation (33) at $x = 0$ and $t = 0$ the pressure ratio is determined by the sum of the A_n coefficients only. Since the initial pressure ratio should be equal to unity, the error associated with taking the first term only is equal to 1.6%. With growing time t, convergence improves because the second and subsequent terms are more suppressed than the first one. Therefore for the calculation of the pressure drop with time during blowdown the first term in Equation (33) is sufficient and hence at $x = 0$,

$$P / P_i = \exp(-\kappa\alpha_1^2 t / L^2) \quad \ldots\ldots\ldots\ldots\ldots (36)$$

Normalizing time t by the constant τ_p, where

$$\tau_p = L^2/\kappa\alpha_1^2 \quad \ldots\ldots\ldots\ldots\ldots\ldots\ldots (37)$$

an exponential expression identical to Equation (11) is obtained:

$$P / P_i = \exp(-\bar{t}) \quad \ldots\ldots\ldots\ldots\ldots\ldots\ldots (38)$$

but containing a different normalization time constant τ_p. Note that from Equations (6), (28), (32) and (37), $\lim_{a\to 0}\tau_p = \tau_v$, and that for $a > 0$, $\tau_p > \tau_v$, indicating that friction

TABLE 2
Gas Composition

Component	Mole %
Methane	91.63
Ethane	4.55
Propane	1.12
i-Butane	0.16
n-Butane	0.21
i-Pentane	0.05
n-Pentane	0.07
Nitrogen	1.78
Carbon-dioxide	0.43

TABLE 3
Gas Properties @ 10°C
(from BWRS with C_{po} data from Aly & Lee, 1981)

Pressure [kPa]	Sound Speed [m/s]	k
8000	399.33	1.4600
6000	395.95	1.3679
4000	398.96	1.3176
2000	406.42	1.2966
1000	411.29	1.2936
100	416.14	1.2941

attenuation in the main pipe tends to increase the blowdown time.

The normalized time of sonic venting can be calculated introducing Equation (10), and hence the dimensional time t_c from

$$t_c = \bar{t}_c \cdot \tau_p \quad \ldots\ldots (39)$$

Numerical Pipe Solution

The same one-dimensional unsteady gas flow equations are used here, again neglecting the inertial terms in the momentum equation, i.e.

$$\text{continuity: } \frac{\partial \rho}{\partial t} + \frac{\partial Q}{\partial x} = 0 \quad \ldots\ldots (40)$$

$$\text{momentum: } \frac{\partial P}{\partial x} + \frac{fQ|Q|}{2\rho D} = 0 \quad \ldots\ldots (41)$$

combined with the state equation [Equation (2)] and the assumptions of isothermal flow along the pipe [Equation (18)] and isentropic expansion through the blowdown stack. This yields a set of non-linear, first-order parabolic partial differential equations for the dependent variables P and Q. An Euler implicit finite difference scheme has been used to obtain the solution. This scheme is known to be first-order accurate in time and second-order accurate in space (Anderson et al., 1984). A typical two-dimensional grid is used with the previously noted boundary conditions: (1) zero flux at $x = 0$; and (2) a flux at $x = L$ which depends on the stack throat area, C_d coefficient, and the line pressure via real gas isentropic expansion to sonic and then subsonic discharge.

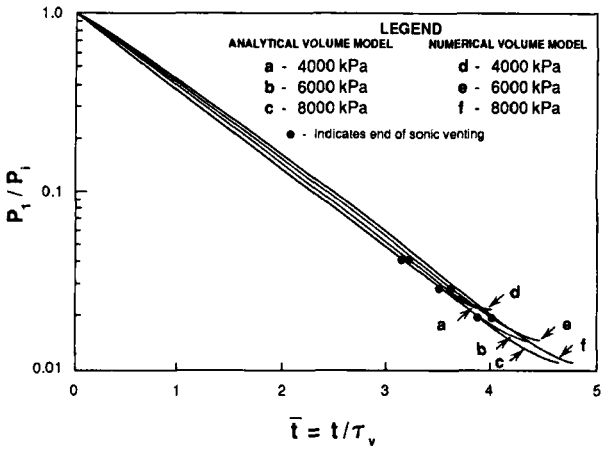

Figure 2 - Pressure-time profiles from analytical and numerical volume models (without stack losses).

Thus, for each time step, Δt, a system of $2n$ (where n is the number of nodes dividing the pipe section) non-linear algebraic equations are formulated from the implicit finite difference scheme. These equations are solved simultaneously using Newton's method. A distinct advantage of this scheme is that the solution is generally stable for all choices of Δt and Δx and it is relatively simple to implement. In addition, the formulation of a straight section of a pipeline results, naturally, in a block-tridiagonal system of equations for which the Thomas algorithm described in Rosenberg (1969) can be applied quite readily. Note that the blocks in this tridiagonal system are 2x2 since the number of dependent variables is two. In the case of complicated piping networks, this block triagonal property is no longer in effect, and a technique based on a sparse variant of Gaussian elimination for sparse systems of equations is used (Duff, 1980).

Example Of Pressure-Time Computations

Computations for the above models and solution methods were performed on an example blowdown of a straight section of pipe through one riser at the end (see Figure 1). The cross-sectional areas involved in this example are: $A_p = 0.8623$ m^2, $A_s = 0.0729$ m^2 and $A_{th} = 0.0498$ m^2. The gas composition used is given in Table 2 and the corresponding gas properties at 10°C are given in Table 3. The results are presented in a normalized form for general application.

Figure 2 shows a comparison between the two methods of solution for the volume model, namely the analytical and mumerical methods for three differenct initiall pressures, P_i = 4000, 6000 and 8000 kPa. The time is normalized with respect to τ_v[see Equation (6)]. The reference gas properties in τ_v were taken as the average values during the blowdown and these are: $c = 404$ m/s for all P_i cases and $k = 1.300$, 1.314 and 1.350 corresponding to $P_i = 4000$, 6000, and 8000 kPa, respectively [see Table 3]. As a result, the analytical solution gives only one profile of the dimensionless pressure up to the end of sonic discharge independent of the initial pressure. The termination points indicating the end of sonic venting are different, naturally, for the different initial pressures. Three different profiles corresponding to the three initial pressures resulting from the numerical solution are also shown in the same figure. This figure illustrates clearly the effects of accounting for real gas behavior and the variations of the gas properties during blowdown. Clearly, the discrepancy between the analytical and the numerical profiles increases as the initial line pressure increases. For example, at $\bar{t} = 3.0$, the

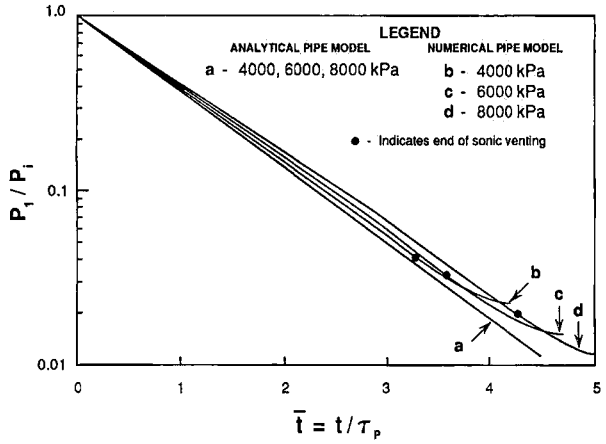

Figure 3 - Pressure-time profiles from analytical and numerical pipe models (without stack losses).

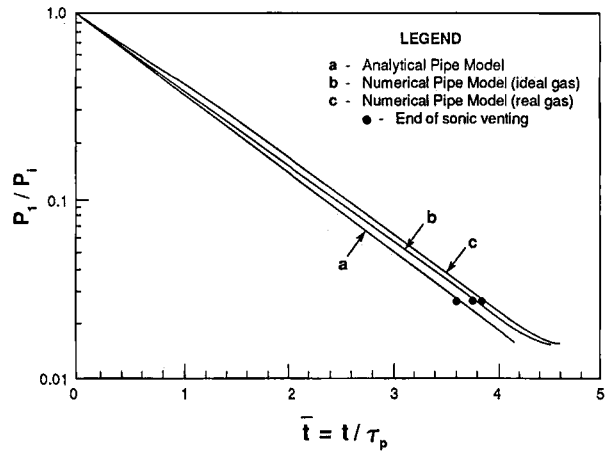

Figure 4 - Effect of real vs. perfect gas equations of state on pressure-time profile for numerical pipe model (P_i = 6000 kPa).

analytical solution gives only one value for P_1/P_i = 0.05 regardless of the initial pressure, while the numerical solution gives P_1/P_i = 0.0515, 0.056 and 0.059 for P_i = 4000, 6000 and 8000 kPa, respectively. It should be emphasized here that since the model equations are the same for both methods, the above discrepancy is attributed only to the variation in the real gas properties in the numerical method with pressure declining during blowdown.

Figure 3 shows a similar comparison between the analytical and numerical solutions for the pipe model, for the three initial pressures of 4000, 6000 and 8000 kPa. The time in this model is normalized with respect to τ_p [see Equation (37)]. The reference gas properties (c and k) used in τ_p are the same as used in τ_v while the main pipe attenuation parameter $a = (fu/2D)_{av}$ was determined from the expression (Osiadacz, 1987)

$$a = \frac{(f/3D)\,[u^2(L) + u(L) \cdot u(O) - u^2(O)]}{[u(L) - u(O)]} \quad \ldots\ldots (42)$$

For sonic venting in the present example, $u(L)_{av}$ was calculated as 13 m/s, f = 0.01, D = 1.048 m and hence a = 0.0415. In the analytical solution, the sonic boundary condition was extended for the subsonic range, as an approximation. This approximation is because an analytical solution is not possible with the introduction of the subsonic boundary conditions. The associated error of this approximation will be given later. The profiles shown in Figure 3 demonstrate the combined

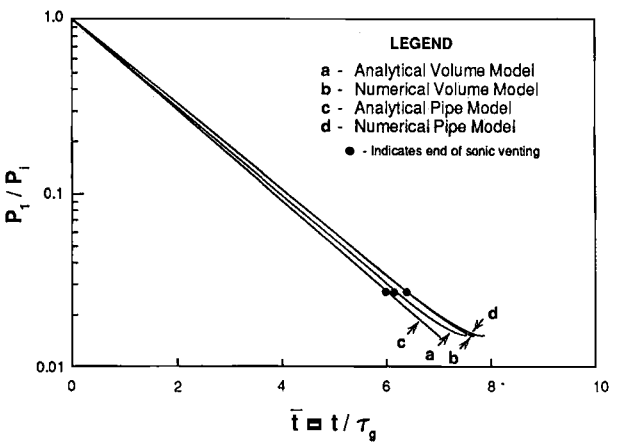

Figure 5 - Pressure-time profile comparison for P_i = 6000 kPa (without stack losses).

effects of both the real gas behavior and the mathematical difference in the methods of solution. In order to quantify the relative contribution of these effects, the numerical computation was run twice for P_i = 6000 kPa using the perfect gas equation of state and the real gas equations, respectively. The results are compared with the analytical solution in Figure 4.

Finally, and in order to give an overall comparison of the two models (volume vs. pipe) and the corresponding methods of solution (analytical vs. numerical), the results of Figures 2 and 3 were plotted in Figure 5. Only the initial pressure case of 6000 kPa is presented and the time is normalized according to the following general normalization:

$$\bar{t} = t / \tau_g \quad \ldots\ldots (43)$$

where τg is a general time constant defined by

$$\tau_g = \left(\frac{L}{c}\right)\left(\frac{A_p}{A_{th} \cdot C_d}\right) \quad \ldots\ldots (44)$$

Notice that the analytical solutions are no longer straight lines on the semi-log graph from the initial conditions to sonic discharge due to the difference in time normalization. Comparing the results of Figure 5 shows that the pressure-time profile obtained from the analytical volume model is below that obtained from the numerical volume model. This is attributed mainly to the effect of real gas behavior. In addition, the volume model solutions generally underpredict the blowdown time due to the lack of attenuation resulting from friction along the main pipe.

Effects Of Stack Losses

In the above analyses, the flow through the stack was assumed isentropic, i.e. stack entrance and friction losses along the length of the stack were neglected. In order to assess the effect of this simplification the entrance loss and friction along L_{s1} were taken into account. Pressure recovery downstream of the throat and friction along L_{s2} were omitted as before. According to the discussion given in the Introduction, pressure recovery enhances the discharge by extending the sonic phase but the loss along L_{s2} lowers the discharge rate during the subsonic phase. The pressure-time profiles already calculated indicate that the subsonic phase constitutes typically about 20% of the total blowdown time, but the corresponding pressure drop is only 1-2.5% of the initial pressure level. In other words during the subsonic phase the pipe pressure drops by less than 100 kPa. These notions

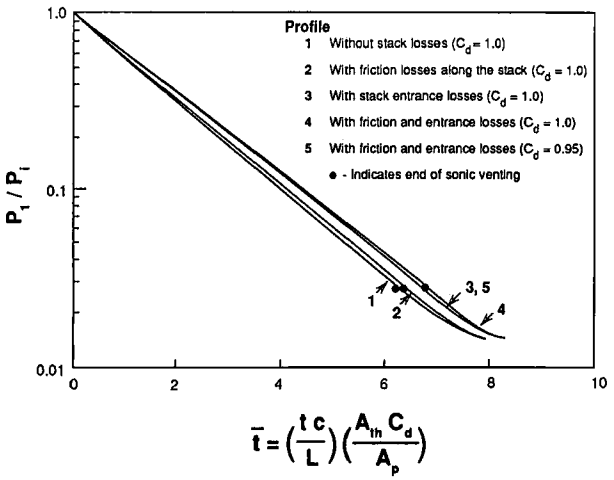

Figure 6 - Pressure-time profiles from numerical pipe model with stack losses (time nomalized w.r.t. τ_g).

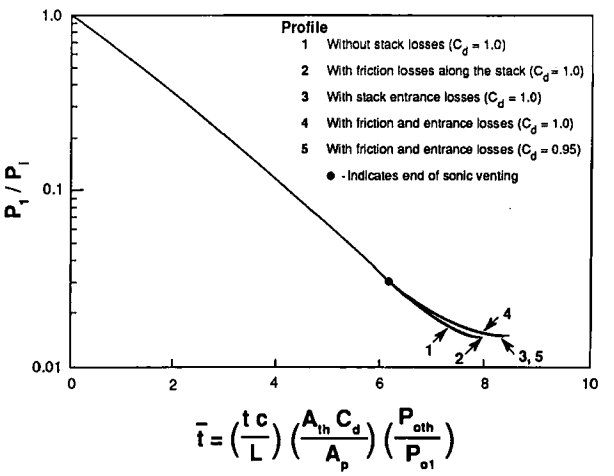

Figure 7 - Pressure-time profiles from numerical pipe model with stack losses (time normalized w.r.t. ($\tau_g \bullet P_{o1} / P_{oth}$)).

imply that for a typical stack characterized in the Introduction the processes occurring downstream of the throat can only change the blowdown history insignificantly. Therefore, the throat was still regarded as an exit to the atmospheric pressure. Most probably the errors in determination of the entrance loss, friction factor along L_{s1} and valve discharge coefficient will have a much stronger effect on the total blowdown time than this simplifying assumption.

Additionally, since the stack is normally short the frictional flow along it can be assumed adiabatic. The energy equation for unsteady compressible gas flow in one-dimensional constant area ducts (streamwise viscous and conductive effects being neglected) can be written as follows (Issa and Spalding, 1972);

$$\frac{\partial}{\partial t}\left[e + \frac{u^2}{2}\right] + \frac{\partial}{\partial x}\left[u\left(e + \frac{P}{\rho} + \frac{u^2}{2}\right)\right] = q \quad \ldots\ldots (45)$$

where q represents the rate of heat transfer per unit mass of the gas and is identically zero for adiabatic flow. Introducing the continuity equation, Equation (22), and the full momentum equation, Equation (23), the above energy equation after some manipulation becomes (Picard and Bishnoi, 1988):

$$\frac{\partial P}{\partial t} + u\frac{\partial P}{\partial x} - c^2\left(\frac{\partial \rho}{\partial t} + u\frac{\partial \rho}{\partial x}\right) = \frac{f\left(\frac{\partial P}{\partial T}\right)_v u^2 |u|}{2 D C_v} \quad \ldots\ldots (46)$$

This energy equation, Equation (46), along with the continuity equation, Equation (22), and the original momentum equation, Equation (23), constitute a set of non-linear hyperbolic partial differential equations. This was solved by the general implicit finite difference scheme of Beam and Warming (1976).

As for the entrance losses at the stack inlet, a quasi-steady flow can be assumed at each time step of the numerical solution. The following equations can then be applied:

$$\text{continuity: } \rho_1 u_1 A_p = \rho_2 u_2 A_2 \quad \ldots\ldots (47)$$

and

$$\text{pressure loss equation: } P_{o1} - P_{o2} = \xi\frac{1}{2}\rho_2 u_2^2 \quad \ldots\ldots (48)$$

where ξ is the entrance loss coefficient (ξ = ½ for sharp-edged entrance), and P_{o1} and P_{o2} are stagnation pressures at sections 1 and 2, respectively (see Figure 1). Again, as a good approximation, the following expressions can be used for the stagnation pressures:

$$P_{o1} = P_1\left[1 + \frac{k_1 - 1}{2}\left(\frac{G_1}{\rho_1 A_p c_1}\right)^2\right]^{\frac{k_1}{k_1 - 1}} \quad \ldots\ldots (49)$$

$$P_{o2} = P_2\left[1 + \frac{k_2 - 1}{2}\left(\frac{G_2}{\rho_2 A_2 c_2}\right)^2\right]^{\frac{k_2}{k_2 - 1}} \quad \ldots\ldots (50)$$

where the values for k_1, k_2, c_1 and c_2 are evaluated for the real gas from the state equation at the conditions of sections 1 and 2, respectively.

Combining the above formulation with the numerical solution for the main pipe model, the blowdown pressure-time profiles were obtained for the stack geometry shown in Figure 1. Figure 6 shows the effects of accounting for stack friction losses and for the entrance losses (ξ = 0.5), separately and combined. Notice that these losses, particularly the entrance losses, increase the blowdown time. Profiles (1) through (4) of Figure 6 are for C_d = 1.0. In this particular example, accounting for friction along the stack increased the blowdown time by 1.5%, while sharp-edged entrance losses increased it by 6.5% and the combined losses by 8%, approximately. Profile 5, however, shows the effects of both losses combined but for C_d = 0.95. It is interesting to see that the dimensionless blowdown time, as defined in Equation (43), for C_d = 0.95 is less than that for C_d = 1.0 (profile 4). This is because the discharge flow rate is lower for C_d = 0.95 which in turn reduces the effects of the stack friction and entrance losses.

In addition, if the time is normalized in a way to allow for these losses, that is

$$\bar{t} = \left(\frac{t \cdot c}{L}\right) \cdot \left(\frac{A_{th} \cdot C_d}{A_p}\right)\left(\frac{P_{oth}}{P_{o1}}\right) \quad \ldots\ldots (51)$$

where P_{oth} is the throat stagnation pressure, all the profiles of Figure 6 collapses to one during the sonic discharge as shown in Figure 7. The subsonic discharge pressure-time profiles,

TABLE 4
Comparison of Results

	L = 1 km						L = 20 km					
P_i (kPa)	4000		6000		8000		4000		6000		8000	
Time (sec) / Method	t_c	t_b	t_c	t_b	t_c	t_b	t_c	t_b	t_c	t_b	t_c	t_b
Volume Model												
– analyitical	234	292	264	322	286	343	4687	5834	5281	6440	5710	6897
– numerical	237	296	271	330	296	356	4731	5920	5419	6609	5933	7121
Pipe Model												
– numerical	227	270	254	297	271	315	4661	5542	5226	6111	5575	6470
– analytical	240	298	272	330	292	351	4910	6170	5570	6850	5970	7290
– numerical with stack losses	247	321	284	352	312	380	5072	6631	5841	7400	6412	7971
– charts in Gradle (1984) without stack losses	–	320	–	340	–	370	–	5800	–	6300	–	6800
– charts in Gradle (1984) with stack losses	–	341	–	362	–	394	–	6180	–	6720	–	7250

however, deviate from each other as the discharge flow is not directly proportional to the stagnation pressure during the subsonic phase.

Comparison Of Results

In order to assess the effects of the models and methods of solution on blowdown time some computations were performed. The results are tabulated in Table 4 which also contains respective results using the charts in Gradle (1984).

Geometry and computation parameters used here are those given in the previous examples. The stack length L_s was taken as 3 m for friction loss calculations, while C_d was assumed unity. The time of sonic venting, t_c, and total blowdown time, t_b, to a line pressure 1% above atmospheric pressure were calculated for three values of P_i and pipe lengths of 1 km and 20 km. The results are tabulated in Table 4.

Examination of Table 4 indicates that the real gas properties (in the numerical solution) increase t_c and t_b by 1-4% in the volume model. In the pipe model the dicrepancy between analytical and numerical solutions increases to 5-7% for t_c. For t_b calculations, however, the numerical pipe solution gives values 9-11% higher than those predicted with the analytical method. This is because the sonic boundary conditions were extended for the subsonic region in the analytical model to allow for integration of the equation as mentioned before.

Table 4 also shows the effects of stack entrance and friction losses. The entrance losses were taken with the maximum ξ value equal to 0.5 corresponding to a sharp-edged entrance. With this value of ξ, stack losses tend to increase both t_c and t_b by a maximum of 6-8%.

Due to the poor resolution of the charts in Gradle (1984), the evaluated t_b is rather inaccurate but generally is about 3-7% longer for the short pipeline and 3-6% shorter for the longer pipeline as compared to the numerical pipe model. The charts also give a consistent 6.5% increase in t_b due to stack losses.

Generally, the above-mentioned discrepancies between the analytical and numerical solutions in the two models depend on the values of c, k and the attenuation factor a used with the analytical solutions. These parameters are determined with some tolerance and thus higher or lower discrepancies are possible. In addition, these discrepancies depend on two main parameters, namely: fL/D and $A_p/(A_{th} \cdot C_d)$. The discharge coefficient C_d depends primarily on the flow contraction coefficient resulting from valve geometry and is normally provided by the valve manufacturer. Figure 8 shows clearly the effects of these two parameters on the sonic blowdown time for example. The results are presented in terms of the ratio of the sonic blowdown time from the different models to that obtained from the numerical pipe model. It is demonstrated in these figures that the discrepancy increases as fL/D increases or $A_p/(A_{th} \cdot C_d)$ decreases.

Comparison With Field Measurements

Field measurements were taken during blowdown of a gas pipeling section in NOVA CORPORATION OF ALBERTA's gas transmission system. Particulars of this section are:

D_p = 0.203 m	P_i = 4089 kPa
D_s = 0.097 m	T_i = 302 K
A_{th} = 0.00548 m2	ξ = 0.2
L_{s1} = 1.3 m	Gas Composition (Table 2)
L_{s2} = 0.7	k= 1.298 at P = 2000 kPa,T = 302 K
L = 25523 m	c = 420 m/s at P = 2000 kPa, T = 302 K

Figure 9 shows the measured P-t profile in the main pipe at section 1 (see Figure 1). Since the diameter of the main pipe section is small in this example, it was appropriate to first match the measured P-t profile with that obtained from the numerical pipe model in order to evaluate the missing value of the discharge coefficient. This C_d was found to be 0.75 which gave a good agreement between the measured profile and that obtained from the numerical pipe model. This value of C_d seems quite reasonable for a plug valve when compared

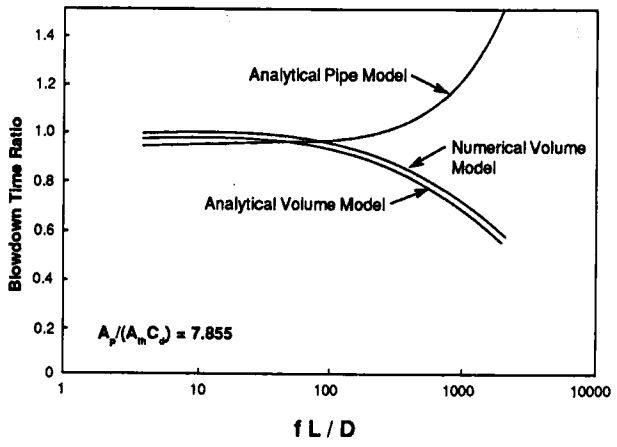

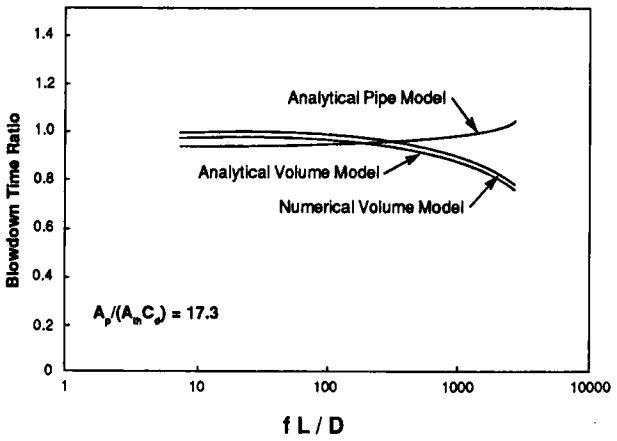

Figure 8 - Ratio of sonic venting blowdown time of various models with respect to numerical pipe model

to 0.73 for choked sharp-edged orifice with zero velocity of approach (Shapiro, 1953 - page 100). The friction factor was calculated at each time step for each discretized section of the pipe as a function of Reynolds number and relative pipe roughness = 1.5 x 10^{-4}. Entrance and friction losses in the stack are both accounted for in the computation. Notice in particular the sharp pressure decrease at the beginning of the blowdown and the ability of the model to simulate this. This sharp pressure decrease is primarily due to the relatively high ($A_{th}C_d/A_p$) resulting in a pronounced transient effects immediately after the opening of the blowdown valve.

The same value of C_d (= 0.75) was used in the other models and the respective profiles are also shown in Figure 9. Notice, the huge discrepancies in both volume models (analytical and numerical) in estimating the *P-t* profile. This is mainly due to the fact that for such a large value of fL/D, the physical model in this case falls short of representing the gas expansion/flow in the pipe. For the analytical pipe model, the attenuation factor a estimated using Equation (42) was = 0.676 (in this example $u(L) = 30$ m/s and $f = 0.0134$) and hence the constant aEL = 3.873. With such large constant (> 0.1), certainly the first term of Equation (33) will not be sufficient as was assumed before, particularly at $x = L$ and $t = 0$. The first six terms were therefore taken in Equation (33) and the corresponding α_n from Carslaw and Jaeger (1959) and A_n from Equation (34) were calculated. Profile 'C' of Figure 9 shows the results of taking these six terms while profile 'd' shows the results of the first term only [i.e., $A_1 \cos(\alpha_1) \exp(-\kappa\alpha_1 t/L^2)$]. It is interesting to see that even with such large

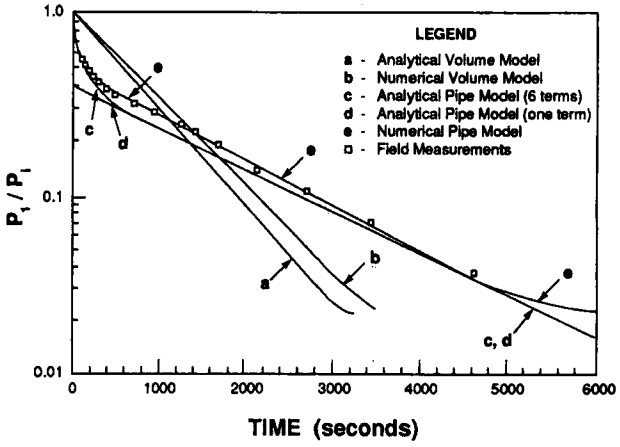

Figure 9 - Pressure- time profile comparison with Field Measurements of a straight pipe section blowdown (fL/D = 1685).

discrepancy at $t = 0$, the two profiles coincide as time elapses, and approach the measured results.

Another field measurement was taken during blowdown of a three-unit compressor station also in the NOVA CORPORATION OF ALBERTA gas transmission system. Station configuration and dimensions are shown in Figure 10. Other particulars are:

D_s = 0.2476 m	P_i = 6042 kPa
A_{th} = 0.0301 m^2	T_i = 292 K
L_{s1} = 1.829 m	Gas Composition (Table 2)
L_{s2} = 1.295 m	k = 1.314 at P = 3000 kPa, T = 292 K
ξ = 0.2	c = 410 m/s at P = 3000 kPa, T = 292 K

Figure 11 shows the measured *P-t* profile at point '*x*' very close to the blowdown stack (see Figure 10). Similarly, for best match of the measured profile to that obtained from the numerical pipe model C_d = 0.87 was used in the model. The transient flow through the orifice plates, check and globe valves and other elements was accounted for in the simulation but are not discussed here in detail due to space limitation of this paper. In this particular example, the C_d = 0.87 is a surprisingly high value probably due to different geometry of the stack valve, and also due to the fact that the system is composed of many throttling elements. These throttling elements were assumed fully open in the simulation, where in reality this may not be the case. As such, error in underestimating local resistances can lead to higher pressure at point '*x*', and hence a fictitiously higher C_d value would be required to match the measured *P-t* profile. The results obtained from all models except the analytical pipe model (which is not possible to obtain due to complexity of the station configuration) are presented for comparison. It is also evident in this case study that the volume (analytical and numerical) models fall short in predicting the blowdown profile and time.

Conclusions

Analytical and numerical analysis verified against field measurements on a pipeline section enabled evaluation of the validity of the volume and pipe models and the effects of friction losses.

It was found that the accuracy of the results obtained from the various models and solution methods depend greatly on the fL/D ratio of the pipe section under blowdown and the stack relative size with respect to the main pipe size. Generally as fL/D increases, predictions using all models except the

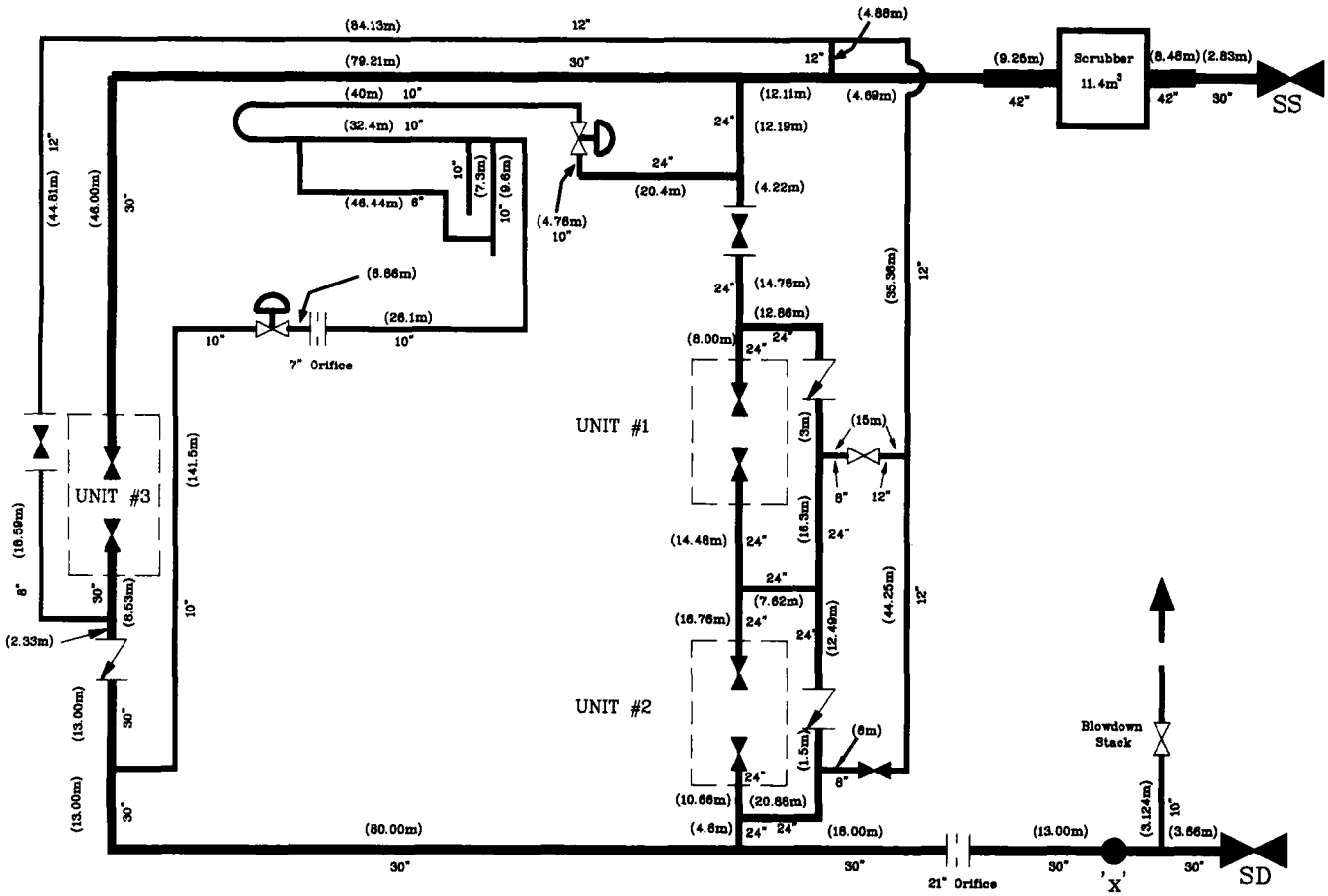

Figure 10 - Compressor station yard piping configuration (numbers in brackets indicate lengths in meters).

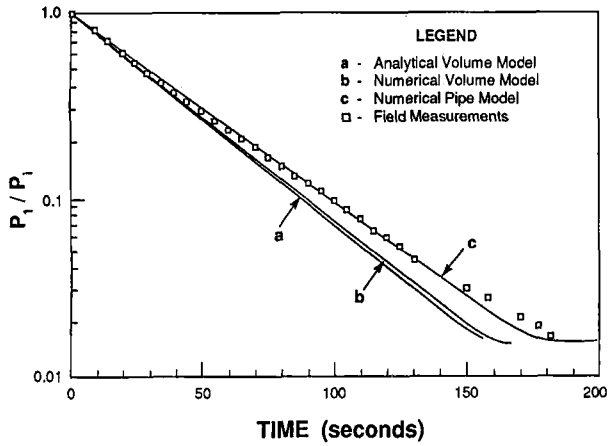

Figure 11 - Pressure-time profile comparison with field measurements during blowdown of the compressor station shown in Figure 10.

numerical pipe model tend to become inaccurate. However, for relatively low fL/D values, all models provide reasonable predictions and therefore the simple analytical volume calculations can be used effectively.

A case study (with fL/D = 1,685) involving field measurements showed that both the analytical and numerical volume models fall short in predicting the P-t profile and the blowdown time. The same conclusion can be drawn from another case study involving field measurements of blowdown of a complicated network of a three-unit compressor station yard piping. The relatively large value of fL/D for the first case study necessitated taking more than just the first term in the series solution of the analytical pipe model in order to better predict the P-t profile.

Finally, it should be emphasized that the precision in estimating the blowdown time greatly depends on the accuracy of the input data used in the simulation particularly the pipe and riser geometry, friction loss and discharge coefficients, and real gas properties.

Acknowledgement

The work presented here is part of a research project sponsored by NOVA CORPORATION OF ALBERTA and the permission to publish it is hereby acknowledged. The authors also acknowledge the valuable comments made by one of the reviewers.

Nomenclature

a	= pipe attenuation factor
A	= pipe cross-sectional area
A_i, B_i	= constants, i = 1, 2, ...n
c	= speed of sound
C_d	= stack valve discharge coefficient
C_{po}	= specific heat at constant pressure (at normal pressure and temperature conditions)
C_v	= specific heat at constant volume
D	= pipe inside diameter
e	= internal energy per unit mass
E	= constant of dimension [Q/P]
f	= Moody friction factor
f	= function of, i.e. f(.....)
G	= gas mass flow rate
k	= gas isentropic exponent
L	= total pipe length
L_s	= total stack length
L_{s1}	= stack length from entrance to valve

L_{s2} = stack length from valve to exit
M = Mach number
N = value of an integral
P = static pressure
$\bar{P}$ = dimensionless pressure
P_{oi} = stagnation pressure at section i
q = rate of heat transfer per unit mass of the gas
Q = gas flux; $Q = \rho u$
R = gas constant
t = time
$\bar{t}$ = dimensionless time = t/τ
T = absolute temperature
u = gas mean velocity in the x-direction
V = volume
x = axial distance

Greek letters

α = dimensionless constant
γ = specific heat ratio
Δ = variable increment
κ = constant defined by Equation (28)
Δ = constant with dimension $[L]^{-1}$
ξ = pressure loss coefficient
ρ = gas density
τ = time constant

Subscript

a = ambient
av = average
b = total blowdown
c = sonic venting
e = exit
g = general
i = initial
p = pressure or pipe
s = subsonic venting, or stack, or entropy
$s1$ = stack, upstream of valve
$s2$ = stack, downstream of valve
th = throat
v = volume or specific volume
0 = condition at closed end of pipe (see Figure 1)
1 = condition at stack end of pipe (see Figure 1)
2 = condition at stack bottom (see Figure 1)

References

Aly, F.A. and L.L. Lee, "Self-Consistent Equations for Calculating the Ideal Gas Heat Capacity, Enthalpy and Entropy", Fluid Phase Equilibria **6**, 169-179 (1981).

Anderson, D.A., J.C. Tannehill and R.H. Pletcher, "Computational Fluid Mechanics and Heat Transfer", Hemisphere Publishing Corp., New York (1984).

Anderson, J.S. and G.E.A. Meier, "Steady and Non-Steady Transonic Flow in a Duct with a Sudden Enlargement", Max-Planck-Institut für Strömungsforschung in Göttingen, Report 1 (1982).

Beam, R.M. and R.F. Warming, "An Implicit Finite-Difference Algorithm for Hyperbolic Systems in Conservation Law Form", J. Comp. Phys. **22**, 87-110 (1976).

Carslaw, H.S. and J.C. Jaeger, " Conduction of Heat in Solids", Second Edition, Oxford Press, London (1959).

Cronje, J.S., P.R. Bishnoi and W.Y. Svrcek, "The Application of the Characteristic Method to Shock Tube Data that Simulate a Gas Pipeline Rupture", Can. J. Chem. Eng. **58** 289-294 (1980).

Duff, I.S., "MA28 - A Set of FORTRAN Subroutines for Sparse Unsymmetric Linear Equations", Computer Science and Systems Division AERE Harwell, **R.8730**, Oxfordshire, England (1980).

Flatt, R., "Unsteady Compressible Flow in Long Pipelines following a Rupture", Int. Journal for Numerical Methods in Fluids **6**, 83-100 (1986)

Gradle, R.J., "Design of Gas Pipeline Blowdowns", Energy Processing Canada, 15-20, January - February (1984).

Groves, T.K., P.R. Bishnoi and J.M.E. Wallbridge, "Decompression Wave Velocities in Natural Gases in Pipe Lines", Can. J. Chem. Eng. **56**, 664-668 (1978).

Harwell Subroutine Library, DC03 Routine, Computer Science and Systems Division of AERE, Harwell Laboratory, Oxfordshire, England (1988).

Issa, R.I. and D.B. Spalding, "Unsteady One-Dimensional Compressible Frictional Flow with Heat Transfer", J. Mech. Eng. Sci. **14** (6), 365-369 (1972).

Jungowski, W.M., "Investigation of Flow Pattern Boundary Conditions and Oscillation Mechanism in a Compressible Flow Through Sudden Enlargement of a Duct", Warsaw Technical University Publication, No. 3 Mechanika (1968).

Osiadacz, A., "Simulation of Transient Gas Flows in Networks", Int. Journal for Numerical Methods in Fluids **4**, 13-24 (1984).

Osiadacz, A., "Simulation and Analysis of Gas Networks", Gulf Publishing Company, Houston, Texas (1987).

Picard, D.J. and P.R. Bishnoi, "The Importance of Real-Fluid Behavior and Nonisentropic Effects in Modeling Decompression Characteristics of Pipeline Fluids for Application in Ductile Fracture Propagation Analysis", Can. J. Chem. Eng. **66**, 3-12 (1988).

Rachford, H.H. Jr. and T. Dupont, "Some Applications of Transient Flow Simulation to Promote Understanding the Performance of Gas Pipeline Systems", SPE Journal, 179-186 (1974).

Shapiro, A.H., "The Dynamics and Thermodynamics of Compressible Fluid Flow", **I**, Ronald Press Company, New York (1953).

Streeter, V.L. and E.B. Wylie, "Natural Gas Pipeline Transients", Society of Petroleum Engineering SPE Paper No. **2555** (1970).

Studzinski, W., M.H. Weiss and K.K. Botros, "Critical Flow Factor for Natural Gas", 2nd International Conference on Flow Measurement, London, U.K., May 11-13 (1988).

Von Rosenberg, D.U., "Methods for the Numerical Solution of Partial Differential Equations", American Elsevier Publishing Co., New York (1969).

Manuscript received September 21, 1988, revised manuscript received February 15, 1989; accepted for publication February 22, 1989.